Inclusive observables calculated with the nuclear random walk model: Application to the $^{40}Ar + {}^{68}Zn$ reaction at 14.6 and 27.6 MeV/nucleon

A. J. Cole
Institut des Sciences Nucléaires, 38026 Grenoble, Cédex, France
(Received 25 June 1986)

A model for peripheral heavy ion reactions which includes, in a consistent formalism, both primary and secondary phases of the reaction mechanism is described. The model is based on a "nuclear random walk" in the projectile-like fragment mass which depends on the number of collisions between projectile and target nucleons along the classical trajectory of relative motion. Emphasis is placed on simple evaluation of experimental observables. An application to the $^{40}Ar+{}^{68}Zn$ reaction, at 14.6 and 27.6 MeV/nucleon, is made and differences between model predictions and measurements, especially at the higher energy, are discussed.

I. INTRODUCTION

With the advent of medium energy (10–100 MeV/nucleon) heavy ion accelerators, a considerable quantity of data on the inclusive production of projectile-like fragments has been accumulated. Examples of such studies may be found in Refs. 1–6. These data have been analyzed mainly in terms of ablation abrasion models[1,3,4] for the yields, while the energy spectra have often been characterized by the momentum width parameter σ_0 related to the Fermi motion of nucleons removed from the projectile.[7] On the other hand, it has been shown in many works that the natural extension[5] of Goldhaber's work[7] to the prediction of angular distributions fails to agree with the measurements.[1,3,6]

Recently, a nuclear random walk model was proposed[8] in which the result of a nucleus-nucleus collision at a given impact parameter was considered to be the result of a random walk in the projectile mass, the number of "steps" being obtained from a Poisson distribution around the average number of nucleon-nucleon collisions calculated in the optical limit of Glauber's theory.[9,10] The use of the number of nucleon-nucleon collisions as a measure of the reaction strength is also the basis for the calculation of fragment yields recently published by Harvey.[11] In Ref. 8, following Karol,[12] this latter quantity was approximated by a Gaussian function of the impact parameter thus:

$$T(b)=\bar{\sigma}_{\mathrm{NN}}\int_{-\infty}^{\infty}dz\left[\int\rho_1(\mathbf{r}_1)\rho_2(\mathbf{r}-\mathbf{r}_1)d\mathbf{r}_1\right]$$
$$\simeq\frac{K\bar{\sigma}_{\mathrm{NN}}}{(2\pi\sigma^2)^{1/2}}\int_{-\infty}^{\infty}e^{-(b^2+z^2)/2\sigma^2}dz\ , \qquad (1)$$

where $\bar{\sigma}_{\mathrm{NN}}$ is the isospin averaged value of the free nucleon-nucleon cross section at the beam energy considered and the trajectory which describes the relative motion between projectile and target is assumed to be a straight line in the beam (z) direction. The Gaussian approximation, shown by Karol to be valid at large impact parameters, makes use of the constants K and σ, which characterize the projectile target combination. It leads to particularly simple expressions for the fragment mass yields.[8] It also simplifies calculations of angular distributions based on an approximate classical deflection function obtained from a point Coulomb repulsion and a "double folding" nuclear real attractive potential.[8,13] This approach visualizes the deflection of the fragment as a combination of potential deflection and recoil effects (due, as in Ref. 5, to the Fermi motion of the mass removed from the projectile) and is similar in spirit to that used by Van Bibber *et al.*[6] In Ref. 1 preliminary calculations using these simple hypotheses were shown to reproduce quite accurately the form of the angular distributions of projectile-like fragments in the $^{40}Ar+{}^{68}Zn$ reaction at 27.6 MeV/nucleon. An important ingredient of the calculation was the inclusion in the random walk of a probability for the loss of alpha particles from the projectile in addition to those representing inelastic scattering and nucleon pickup and stripping.

It is the purpose of the present work to present a more detailed account of the model and show how one may obtain various experimental observables. Examples of calculations for the $^{40}Ar+{}^{68}Zn$ reaction will be given which reproduce most of the observed features of the data. This reaction was chosen since it seems to be fairly typical of light projectile reactions, but also because of the extent (these data form part of a systematic experimental study) and quality of the measurements.

Before comparing data and calculations we will make a brief presentation of the model and discuss improvements which have to do with geometrical aspects of the profile $T(b)$ which may be influenced by Pauli blocking[14] (Sec. II A). In Sec. II B we present the formalism when alpha particle emission from the projectile is included as a competing probability in the random walk; Sec. II C shows how the improved geometry modifies angular distributions. The important consequences of evaporation from excited fragments after the reaction will also be discussed (Sec. II D). These improvements will clear the way for a discussion of the $^{40}Ar+{}^{68}Zn$ data (Sec. III). An estimation of the average energy loss of projectile-like fragments is included in Sec. III, although in this work no attempt has been made to make detailed calculations of energy spectra. Finally, in Sec. IV we present a summary of our principal results and some concluding remarks.

II. THE NUCLEAR RANDOM WALK MODEL

A. Improvements to the model

The principle of the model is very simple. The Poisson distribution which describes the probability density for exactly n nucleon-nucleon collisions is

$$P_n = \frac{T^n e^{-T}}{n!} , \tag{2}$$

where $T(b)$ is given by Eq. (1). The simplest form of the model states that the consequences of each nucleon-nucleon collision may be described by constant competing probabilities P_{-1}, P_{+1}, and P_0 for single nucleon loss or gain and inelastic scattering. We may then write down the probability for a given mass loss m_l from the projectile at a given impact parameter $b(T)$ as

$$\begin{aligned} P_{m_l}(T(b)) &= \sum_{n,ijk} P_n n! \frac{P_{-1}^i}{i!} \frac{P_{+1}^j}{j!} \frac{P_0^k}{k!} \\ &= \left[\frac{P_{-1}}{P_{+1}} \right]^{m_l/2} \mathrm{Im}_l(2T\sqrt{P_{-1}P_{+1}}) \\ &\quad \times e^{-(P_{-1}+P_{+1})T} , \end{aligned} \tag{3}$$

where I_{m_l} is a modified Bessel function of order $m_l = i - j$ and $n = i + j + k$. Now, using the Gaussian geometry

$$\frac{dT}{T} = -\frac{db^2}{2\sigma^2} , \tag{4}$$

and assuming $m_l \ll (P_{-1} - P_{+1}) K \sigma_{\mathrm{NN}}$, we obtain the differential yield as in Ref. 8:

$$\begin{aligned} \frac{d\sigma}{dm_l} &= \int_0^\infty 2\pi b \, db \, P_{m_l}(T) \\ &\approx 2\pi\sigma^2 \left[\frac{P_{-1}}{P_{+1}} \right]^{m_l/2} \int_0^\infty e^{-(P_{-1}+P_{+1})T} \\ &\quad \times I_{m_l}(2T\sqrt{P_{-1}P_{+1}}) dT/T , \end{aligned} \tag{5}$$

which, by taking advantage of the recursion relationship for modified Bessel functions and substituting $\alpha = (P_{-1} + P_{+1})/2\sqrt{P_{-1}P_{+1}}$, we may rewrite as

$$\begin{aligned} \frac{d\sigma}{dm_l} &= \frac{2\pi\sigma^2}{m_l} \left[\frac{P_{-1}}{P_{+1}} \right]^{m_l/2} \\ &\quad \times \tfrac{1}{2} \int_0^\infty e^{-\alpha x} [I_{m_l-1}(x) - I_{m_l+1}(x)] dx . \end{aligned} \tag{6}$$

Now, choosing $P_{-1} > P_{+1}$ (the projectile loses mass, on the average), we easily obtain that the cross section for losing mass m_l from the projectile is

$$\frac{d\sigma}{dm_l} = \frac{2\pi\sigma^2}{m_l} , \tag{7}$$

whereas that for gaining mass, m_g, is

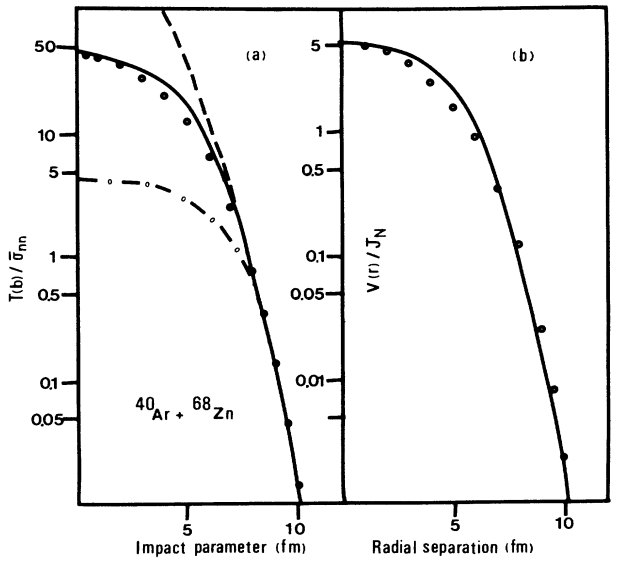

FIG. 1. (a) Variation with impact parameter of the integral along a straight line trajectory of the convolution of the ^{40}Ar and ^{68}Zn matter densities. The solid curve is the exponential integral approximation with $k = 0.0367$. The dashed curve is the Gaussian approximation. The dotted-dashed curve simulates a Pauli suppression factor of 10 ($k = 0.565$). (b) Variation of the convolution of matter densities of ^{40}Ar and ^{68}Zn with the radial separation of their centers. The parameters used to specify the Saxon-Woods forms for the densities are, for ^{40}Ar, $\rho_0 = 0.163$, $r = 3.659$, and $a = 0.515$; and for ^{68}Zn, $\rho_0 = 0.177$, $r = 4.313$, and $a = 0.523$. The solid line was obtained using Eq. (22) ($\beta = 0.2874$).

$$\frac{d\sigma}{dm_g} = \frac{2\pi\sigma^2}{m_g} \left[\frac{P_{+1}}{P_{-1}} \right]^{m_g} . \tag{8}$$

If $P_{+1} > P_{-1}$, of course the cross sections should be exchanged as required by symmetry.

In Fig. 1(a) we show the quantity $T/\bar{\sigma}_{\mathrm{NN}}$ [Eq. (1)] evaluated numerically. The geometrical parameters used in the calculation to specify the Saxon-Woods forms for the densities of ^{40}Ar and ^{68}Zn are given in the figure caption. Also shown in the figure is the Gaussian approximation fitted to the numerical calculation at $b = 8.5$ fm. It can be seen that the approximation is reasonable only for $b > \sim 8$ fm. A considerable improvement may be obtained, however, by using the form

$$\frac{dT}{T} = -\frac{db^2}{2\sigma^2} e^{-kT/\bar{\sigma}_{\mathrm{NN}}} , \tag{9}$$

which leads to the relation between T and b,

$$\frac{b^2}{2\sigma^2} = \mathrm{Ei}\left[\frac{kT(0)}{\bar{\sigma}_{\mathrm{NN}}} \right] - \mathrm{Ei}\left[\frac{kT(b)}{\bar{\sigma}_{\mathrm{NN}}} \right] , \tag{10}$$

where $\mathrm{Ei}(x)$ is the usual exponential integral. We note that for small arguments (small T at large b) we recover the Gaussian form [$\mathrm{Ei}(x) \sim \ln(x) + \gamma$ for small x, where $\gamma = 0.577$ is Euler's constant]. Thus, Eq. (10) has the dou-

ble advantage of maintaining the Gaussian approximation at large impact parameters, while producing a greatly improved description of the geometry of two interpenetrating nuclei at smaller impact parameters.

A possible further advantage of Eq. (9) has to do with the consequences of Pauli blocking. Harvey[11] has attempted to introduce such effects in his calculation of fragment yields by employing an empirical density dependent effective nucleon-nucleon cross section. This procedure leads naturally to a decrease in the average number of nucleon-nucleon collisions for small impact parameters relative to that number calculated using the free value of $\bar{\sigma}_{\rm NN}$. Such behavior can be approximately simulated using Eq. (10), by introducing a Pauli blocking factor (R_P) equal to the ratio of the blocked average number of nucleon-nucleon collisions at zero impact parameter to the unblocked value (obtained using the geometrical convolution and the free nucleon-nucleon cross section). We thus simply reduce the value of $T(0)$ by a factor R_P (increase k). The form of the equation ensures that T will be unchanged for large values of b corresponding to the fact that $\bar{\sigma}_{\rm NN}$ tends to the free value at large separations of projectile and target [Fig. 1(a)]. Thus the most peripheral reactions will be insensitive to the value of R_P, whereas more central reactions will show increased sensitivity. Harvey finds that the inclusion of this effect has little consequence for his calculation of yields. The analytical simplicity of Eq. (9), on the other hand, leads straightforwardly to a modified expression for the yields (compared with that obtained using a Gaussian geometry), as will now be shown. Equation (6) is replaced by

$$\frac{d\sigma}{dm_l}=\frac{2\pi\sigma^2}{m_l}\left[\frac{P_{-1}}{P_{+1}}\right]^{m_l/2} \times\tfrac{1}{2}\int_0^\infty e^{-(\alpha-\gamma)x}[I_{m_l-1}(x)-I_{m_l+1}(x)]dx \ , \tag{11}$$

where

$$\gamma=\frac{k}{2\bar{\sigma}_{\rm NN}\sqrt{P_{-1}P_{+1}}} \ . \tag{12}$$

Using the shift theorem for Laplace transforms and supposing that $\gamma \ll \alpha$ (as is the case in practice), we obtain

$$\frac{d\sigma}{dm_l}=\frac{2\pi\sigma^2}{m_l}\frac{1}{(1-\epsilon)^{m_l}} \ , \qquad \frac{d\sigma}{dm_g}=\frac{2\pi\sigma^2}{m_g}\left[\frac{P_{+1}}{P_{-1}}\right]^{m_g}\frac{1}{(1+\epsilon)^{m_g}} \ , \tag{13}$$

where

$$\epsilon=\gamma/(\alpha^2-1)^{1/2}=k/\bar{\sigma}_{\rm NN}(P_{-1}-P_{+1}) \ . \tag{14}$$

The most important feature of Eq. (13) is that the cross sections are now clearly energy dependent via the energy dependence of $\bar{\sigma}_{\rm NN}$, even if we exclude Pauli blocking effects. Of course, if k is increased from the geometrical value the effects should be more striking. On the other hand, it should be made clear that the rise in cross section probably mainly concerns primary yields. Sequential emission from excited fragments far from the projectile tends to deplete these yields, and thus may stabilize the cross sections with increasing energy.

B. Inclusion of alpha particle emission

The inclusion of alpha particle (or any other particle) emission in the random walk formalism is straightforward. It leads to a simple extension of Eq. (3), which becomes

$$P_{m_l}(T)=\sum_{i,j,k,l}\frac{(P_0T)^i}{i!}\frac{(P_{+1}T)^j}{j!}\frac{(P_{-1}T)^k}{k!}\frac{(P_{-4}T)^1}{1!}e^{-(P_{-1}+P_{+1}+P_0+P_{-4})T}$$
$$=\left[\frac{P_{-1}}{P_{+1}}\right]^{m_l/2}e^{-(P_{-1}+P_{+1}+P_{-4})T}\sum_{l=0}^{\infty}\frac{(TP_{+1}^2P_{-4})^l}{l!}I_{m_l-4l}(2T\sqrt{P_{-1}P_{+1}}) \ , \tag{15}$$

where the index l indicates the number of alpha particles (mass four units in this context) emitted and $m_l=4l+k-j$. The associated cross section may be written

$$\sigma_{m_l}=2\pi\sigma^2\left[\frac{P_{-1}}{P_{+1}}\right]^{m_l/2}\sum_{l=0}^{\infty}\frac{p^l}{l!}\int_0^{2T(0)\sqrt{P_{-1}P_{+1}}}e^{-qx}x^{l-1}I_{m_l-4l}(x)dx \ , \tag{16}$$

where

$$p=\frac{P_{+1}^2P_{-4}}{2P_{-1}^2\sqrt{P_{-1}P_{+1}}} \quad \text{and} \quad q=\frac{(P_{+1}+P_{-1}+P_{-4}-k/\bar{\sigma}_{\rm NN})}{2\sqrt{P_{-1}P_{+1}}} \ .$$

If the upper limit of the integral may be safely set equal to infinity, we obtain

$$\sigma_{m_l}=2\pi\sigma^2\left[\frac{P_{-1}}{P_{+1}}\right]^{m_l/2}\sum_{l=0}^{\infty}\frac{[p/(q^2-1)^{1/2}]^l}{l!}\Gamma(m_l-3l)P_{l-1}^{4l-m_l}[q/(q^2-1)^{1/2}] \ , \tag{17}$$

where P_ν^μ is a Legendre polynomial. It can be shown by using the Fokker-Planck approximation that the use of the infinite upper limit is justified provided that $T(0)(P_{-1}+4P_{-4}-P_{+1})\gg m_l$, a condition which is reasonably satisfied in our calculations [see Sec. III and Fig. 1(a)]. As in Eq. (8), the corresponding expression for m_g can be obtained by substituting $m_g=-m_l$ and using the fact that $I_\nu=I_{-\nu}$.

C. Calculation of angular distributions

The basic ideas underlying the calculation of angular distributions have already been explained in Ref. 8. The differential element $d\sigma=2\pi b\,db$ is converted to a function of the laboratory deflection angle using a classical deflection function derived from a double folding nuclear attraction and a point Coulomb repulsion. The resulting angular distribution which represents the sum of all processes is then multiplied by the probability [Eq. (15)] to produce a given mass deficit. Thus,

$$\frac{d\sigma^{m_l}}{d\Omega_{\rm lab}}=\frac{2\pi b}{2\pi\sin\theta_{\rm lab}}\frac{db}{d\theta_{\rm lab}}P_{m_l}[T(b)]\ . \tag{18}$$

The modified geometry influences the angular distributions partly through the Jacobian db^2/dT and partly by modifying the deflection function. The modification to the Jacobian is immediate:

$$\frac{d\sigma^{m_l}}{d\Omega_{\rm lab}}=\frac{e^{kT/\bar\sigma_{\rm NN}}}{\sin\theta_{\rm lab}}\frac{\sigma^2}{T}\frac{dT}{d\theta_{\rm lab}}P_{m_l}(T)\ . \tag{19}$$

The modification to the deflection function comes about as follows. The nuclear part of the deflection was written in Ref. 8 as

$$\theta_{\rm lab}^{\rm nuc}=\frac{1}{2E_{\rm lab}}\int_{-\infty}^{\infty}-\frac{b}{r}\frac{dV(r)}{dr}dz$$
$$=-\frac{b}{E_{\rm lab}}\int_{-\infty}^{\infty}\frac{dV(r)}{dr^2}dz\ , \tag{20}$$

where

$$V(r)=J_{\rm N}\int\rho_1(\mathbf{r}_1)\rho_2(\mathbf{r}-\mathbf{r}_1)d\mathbf{r}_1 \tag{21}$$

is obtained as the convolution of a zero range nucleon-nucleon potential (with volume integral $J_{\rm N}$ MeV fm^3) with the projectile and target densities.[13]

In Fig. 1(b) we show that the convolution itself is well represented by a function of the same shape as that used to describe the average number of nucleon-nucleon collisions $T(b)$. Thus $V(r)/J_{\rm N}=C(r)$ is approximately given by solving

$$\frac{r^2}{2\sigma^2}=\mathrm{Ei}[\beta C(0)]-\mathrm{Ei}[\beta C(r)]\ , \tag{22}$$

so that

$$\frac{dV(r)}{dr^2}=\frac{-V(r)}{2\sigma^2}e^{-\beta V(r)/J_{\rm N}}\ , \tag{23}$$

and thus

$$\theta_{\rm lab}^{\rm nuc}=\frac{b}{2\sigma^2E_{\rm lab}}\int_{-\infty}^{\infty}V(r)e^{-\beta(V(r)/J_{\rm N})}dz\ . \tag{24}$$

Developing the exponential, we find that the first term is

$$\theta_0=\frac{b}{2\sigma^2E_{\rm lab}}\int_{-\infty}^{\infty}V(r)dz\ , \tag{25}$$

and that the full expression reads

$$\theta_{\rm lab}=\theta_{\rm lab}^{\rm nuc}+\theta_{\rm lab}^{\rm Coul}$$
$$=\theta_0+\frac{b}{2\sigma^2E_{\rm lab}}\sum_{n=1}^{\infty}\frac{(-\beta/J_{\rm N})^n}{n!}$$
$$\times\int_{-\infty}^{\infty}[V(r)]^n dz-\frac{Z_1Z_2e^2}{bE_{\rm lab}}\ , \tag{26}$$

where we have included the repulsion due to a point Coulomb interaction. The first term of Eq. (26) was derived in Ref. 8 using the Gaussian geometry, which results in the simple relations

$$V(r)=\frac{J_{\rm N}}{\bar\sigma_{\rm NN}}\frac{dT}{dz},\quad \theta_0=\frac{bJ_{\rm N}T}{2\sigma^2E_{\rm lab}\bar\sigma_{\rm NN}}\ . \tag{27}$$

In this work we have used this approximation to evaluate the (small) correction terms, but have retained Eq. (25) for the evaluation of θ_0 using $V(r)$ given by Eq. (22). The main result of the modification is to reduce $\theta_{\rm lab}^{\rm nuc}$ for large T and thus increase $dT/d\theta_{\rm lab}$ in Eq. (19).

D. Effect of evaporation

Evaporation (secondary emission) corrections could, of course, be included explicitly using a multistep Hauser-Feshbach code,[15,16] provided that knowledge of primary fragment excitation energies and angular momentum distributions is available. In the absence of detailed knowledge of these distributions, we are justified in formulating an approximate treatment of evaporation. We now show that a reasonable approximation to the results of such calculations, and thus to the measured mass distributions following compound nucleus formation and decay at low energies, may be obtained by once again invoking a random walk process. The mass distribution following evaporation from a compound nucleus is written

$$P_{m_e}=\sum_{n_e}G(n_e)n_e!\frac{P_{\rm N}^{k_e}}{k_e!}\frac{P_\alpha^{l_e}}{l_e!}\ , \tag{28}$$

where n_e is the number of evaporated particles, $m_e=k_e+4l_e$, $n_e=k_e+l_e$, $G(n_e)$ is a normalized Gaussian probability distribution characterized by the width σ_{n_e}, and $P_{\rm N}$ and P_α, represent, respectively, the nucleon and alpha particle emission probabilities. Mass distributions calculated with Eq. (28) are presented with the corresponding data in Fig. 2. They were obtained with $\langle n_e\rangle=E_x/18.4$ MeV, $\sigma_{n_e}=0.25\langle n_e\rangle$, and $P_{\rm N}=P_\alpha=0.5$ for all systems. The description of any given data set may be improved by varying σ_{n_e}. The important point, is, however, that the square of the intrinsic evaporation width remains small compared to $\langle n_e\rangle$. Of course, the data in Fig. 2 are better described by the full multistep

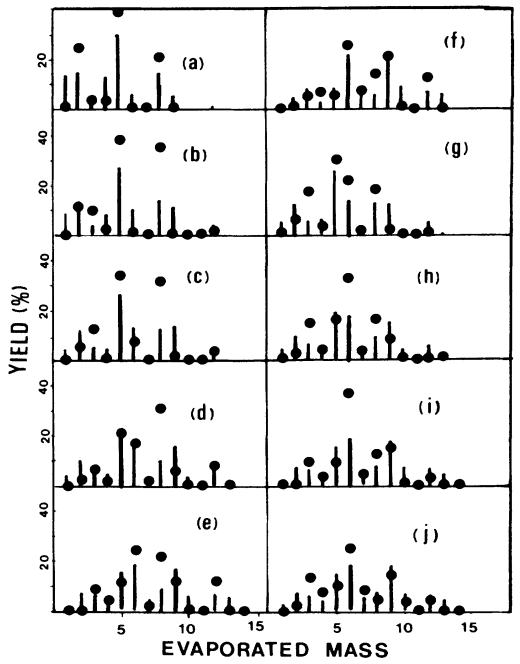

FIG. 2. Results of the random walk equation (28) (vertical bars) compared with measured yields of evaporation residues (solid circles). (a)–(f): $^{16}O+^{16}O$ at $E_{lab}=35$, 45, 52, 60, 70, and 80 MeV (data Ref. 17). (g)–(i): $^{19}F+^{12}C$ at $E_{lab}=50$, 63.2, and 76 MeV (data Ref. 16). (j): $^{16}O+^{27}Al$ at $E_{lab}=60$ MeV (data Ref. 16). The yields are plotted in terms of the number of mass units removed from the compound nucleus.

Hauser-Feshbach calculations. Nevertheless, the almost trivial formula (28) reproduces the main features of the measured distributions.

To apply evaporation corrections to projectile-like fragment distributions we need to make more assumptions concerning the energy dissipation and the sharing of the excitation energy E_x^T between projectile- and target-like fragments. We assume

$$E_x^T=P_0'\langle n_p\rangle E_{lab}/A_p \ , \tag{29}$$

where P_0' is the primary inelastic probability, n_p is the number of primary collisions, and E_{lab}/A_p is the beam kinetic energy per projectile nucleon. If this energy is shared between the primary projectile-like and target-like fragments in proportion to the projectile/target mass ratio (equal temperature assumption), the excitation energy of the projectile is given at small angles by

$$E_x=P_0'\langle n_p\rangle\frac{E_{lab}}{A_p}\frac{A_p}{A_p+A_t} \ , \tag{30}$$

so that, in terms of Eq. (28),

$$\langle n_e\rangle=\frac{P_0'E_{lab}}{18.4(A_p+A_t)}T\equiv P_eT \ , \tag{31}$$

which defines P_e as the evaporation probability (the probability that a primary nucleon-nucleon collision leads to subsequent evaporation of a nucleon or an alpha particle after the primary reaction). Multiplying this evaporation probability by the probabilities that the evaporated particle will be either an alpha particle or a nucleon obtained as described above by fitting evaporation residue mass distributions, we obtain $P_N=P_\alpha=0.5P_e$. It will have been noted that the width induced in the number of evaporated particles due to variation in the number of primary collisions is considerably larger than that of Eq. (28). It follows that we make little error in neglecting the intrinsic evaporation width, in which case we may incorporate the secondary evaporation chain directly in the random walk of Eq. (15). Thus,

$$P_{m_l}(T)=\sum_{\substack{j,k,l\\k_e,l_e}} e^{-(P'_{+1}+P'_{-1}+P'_{-4}+P_N+P_\alpha)T} \times\frac{(P'_{+1}T)^j}{j!}\frac{(P'_{-1}T)^k}{k!}\frac{(P'_{-4}T)^l}{l!} \times\frac{(P_NT)^{k_e}}{k_e!}\frac{(P_\alpha T)^{l_e}}{l_e!} \ , \tag{32}$$

where the primes are meant to designate primary probabilities. By combining terms containing P'_{-1}, P_N and P'_{-4}, P_α, we obtain an equation similar to (15),

$$P_{m_l}(T)=e^{-(P_{-1}+P_{+1}+P_{-4})T} \times\sum_{j,k,l}\frac{(P_{+1}T)^j}{j!}\frac{(P_{-1}T)^k}{k!}\frac{(P_{-4}T)^l}{l!} \ . \tag{33}$$

Equation (33) says that evaporation corrections can be included directly in the random walk formalism, modifying only the probabilities characterizing the random walk. An equivalent statement is that inclusive measurements of mass (charge) distributions of projectile- (target-) like fragments cannot be used to distinguish between primary and secondary (evaporative) emission processes. These statements, of course, remain true if we use some energy partitioning other than Eq. (30). We require only that the excitation energy of the decaying fragment be proportional to the number of nucleon-nucleon collisions.

Constraints on the values of the random walk probabilities may be formulated as follows:

$$\begin{aligned} &P'_{-1}+P'_{+1}+P'_{-4}+P'_0=1 \ , \\ &P_{-1}=P'_{-1}+P_N \ , \\ &P_{-4}=P'_{-4}+P_\alpha \ , \\ &P_N+P_\alpha=P_e=\frac{P_0'E_{lab}}{18.4(A_p+A_t)} \ . \end{aligned} \tag{34}$$

These equations are, however, insufficient to determine the individual probabilities.

We close this section with a comment on Eq. (28). Using this very simple equation we have obtained a reasonable description of fusion-evaporation mass distributions, despite the fact that the competing probabilities for nucleon and alpha particle emission would be expected to vary significantly with the nucleus encountered in the

deexcitation chain. In this sense their values must represent some of the average probabilities. The situation may be similar for the primary emission probabilities; i.e., although these probabilities should vary from nucleus to nucleus and maybe even with the exact position at which the nucleon-nucleon collision takes place, average values which are kept constant succeed in reproducing the main features of the reaction mechanism.

III. ANALYSIS OF THE $^{40}Ar+^{68}Zn$ DATA

The data to be analyzed consist mainly of charge yields ($d\sigma/dz$) obtained between 3° and 30° (lab) at 14.6 and 27.6 MeV/nucleon. The main features of the experiments are described in Refs. 1 and 18. At the higher energy, mass identification was achieved at small angles (3°—7°). The expression for total reaction cross sections using the Gaussian geometry [Eq. (1), valid at large impact parameters] is[12]

$$\sigma_R = 2\pi\sigma^2[\ln(K\bar{\sigma}_{NN})+\gamma] \ . \tag{35}$$

This expression yields values of 3200 and 3050 mb, which agree very well with the experimental values of 3110 and 3000 mb at 14.6 and 27.6 MeV/nucleon, respectively. Since the measured cross sections for fragments between $A_f=21$ and 42, are, respectively, 1690 and 2200 mb, we thus see that a substantial part of the cross section at the higher energy is due to rather central collisions (and/or to events involving multiplicities >1), and therefore will not be described correctly in the present model. The more central collisions are expected to give rise to very highly excited projectile-like fragments (perhaps with temperatures as high as 7 MeV) which subsequently decay. The calculations of Barbagallo *et al.*[19] predict that such nuclei would disintegrate, giving rise to three distinct groups of fragments in the mass ranges A 1—5, 10—18, and 19—35.

The model parameters consist, in principle, of four primary probabilities, P'_{+1}, P'_{-1}, P'_0, and P'_{-4}, the secondary probabilities being determined by Eqs. (29)—(31). We have supposed that alpha particle loss from the projectile-like fragment as a primary process is negligible, so that with the condition $P'_{+1}+P'_{-1}+P'_0=1$ we are left with only two free random walk parameters. A third parameter comes from the rather artificial introduction of the effects of the Pauli principle. This parameter was characterized in Sec. II by the ratio (R_p) of the number of collisions at an impact parameter $b=0$ fm to that number obtained by multiplying the numerical integration of the density convolution [Eq. (1)] by the free nucleon-nucleon cross section, and has been fixed at $R_p=0.1$. Using a constant value of R_p is equivalent to supposing that the Pauli blocking effects do not vary strongly over the energy range considered, a supposition which is supported by the nucleon-nucleus calculations of Hasse and Schuck.[14]

The primary nucleon gain probability would be expected to be rather less than the loss probability P'_{-1}. This is simply because P'_{-1} refers to nucleons which escape from the projectile and are either captured in the target or emerge as free nucleons, whereas P'_{+1} refers to those nucleons which escape from the target and are captured by the projectile.

Consideration of low energy direct reactions leads us to expect that the primary inelastic probability is about 5 times larger than P'_{-1} or P'_{+1}. We have accordingly fixed these parameters as $P'_{+1}=0.1$, $P'_{-1}=0.15$, and $P'_0=1-P'_{-1}-P'_{+1}=0.75$. The secondary emission probabilities are determined by Eqs. (34).

A. Mass and charge yields

As mentioned in Sec. II A, the modified geometry allows us to calculate mass yields [Eq. (17)] either by using a collision profile corresponding to the geometrical convolution or by depressing the number of collisions for small impact parameters. Calculations corresponding to these two cases are shown in Fig. 3. The charge yields were obtained from the calculated mass yields by folding with a Gaussian distribution (corresponding to the observed width in the mass distribution for a given charge) centered about the most probable mass observed for each charge and renormalized by a factor of 2. This normalization is justified by the fact that the observed nuclei, in general, lie close to the stability line.

As expected, the description of the data at the lower en-

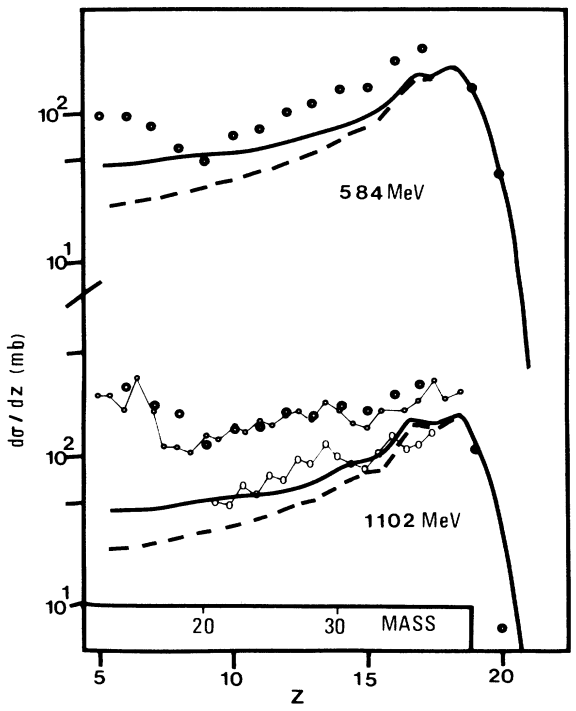

FIG. 3. (a) Measured charge yield in the $^{40}Ar+^{68}Zn$ reaction at 14.6 MeV/nucleon. The calculation (dotted line) is the result of Eq. (17) adapted for charge yields as explained in Sec. III A. The solid line shows the effect of Pauli suppression as described in the text. (b) Same as (a), but at 27.6 MeV/nucleon. The mass yield multiplied by 2 is superimposed on the charge yield. The mass yield corresponding to peripheral collisions (open circles) also multiplied by 2 is also shown in the figure.

ergy is quite good, particularly when the Pauli suppression factor is used. At the higher energies it is necessary to distinguish between the total observed fragment yields and that part of the yield which refers to peripheral collisions (referred to by the authors of Ref. 1 as "quasi-fragmentation"). The magnitude and shape of this part of the fragment yield is quite well reproduced by the calculation (Fig. 3). However, the total yield (shown for both mass and charge) is about a factor of 2 larger. It seems likely that this additional yield can be ascribed to the disintegration of highly excited nuclei produced in more central collisions. Preliminary calculations[20] support this idea. If this conjecture is correct, it means that such reactions can provide good opportunities for studying the decay of hot nuclei. Both the calculations by Barbagallo *et al.*[19] and by Bondorf *et al.*[21] predict that such nuclei may fragment into two or more large pieces, the principal reason being that the ratio of Q value to the temperature, $Q(t)/t$, diminishes with increasing temperature t.

B. Angular distributions

Angular distributions have been calculated in accordance with Eqs. (19) and (26). Since at a given angle the differential cross sections vary smoothly with increasing mass loss from the projectile, the distribution for a given Z has been taken to be that corresponding to the most probable value of m_l (renormalized by a factor of 2). In this calculation Pauli blocking effects were not introduced into the real potential, which thus has the radial profile of the convolution of the projectile and target densities. The reason is that only the energy dependent part of the real potential would be expected to be influenced by such effects, and the total potential is probably dominated by the energy independent (Hartree-Fock) part.[22] In making the calculations it is also necessary to take into account the effects of the recoil due to the missing mass. This was achieved exactly as described in Ref. 8 by folding the calculated angular distributions with a Gaussian whose width is given in Ref. 8 as

$$\sigma_\theta^2=\sigma_G^2/P_F^2 , \tag{36}$$

where P_F is the fragment momentum (corresponding to the beam velocity), and the value of the σ_G parameter has been calculated using a Fermi momentum width parameter $\sigma_0=84$ MeV/c. The effect of the convolution is illustrated in Fig. 4. It will be recalled that Goldhaber[7] has shown that the evolution of σ_G with the final fragment mass A_F,

$$\sigma_G^2=\sigma_0^2 A_F(A_p-A_F)/(A_p-1) , \tag{37}$$

does not depend on whether the mass is removed during or after the interaction.

As seen in Fig. 4, the comparison of the shapes of calculated and measured distributions is extremely satisfactory, even at the higher energy. It depends principally on the ratio of the total nucleon emission probability P_{-1} to the corresponding alpha particle emission probability P_{-4} and thus, in the present context, mainly on the value of P_0'. In particular, the presence of an alpha particle emission probability is responsible for the change in slope near

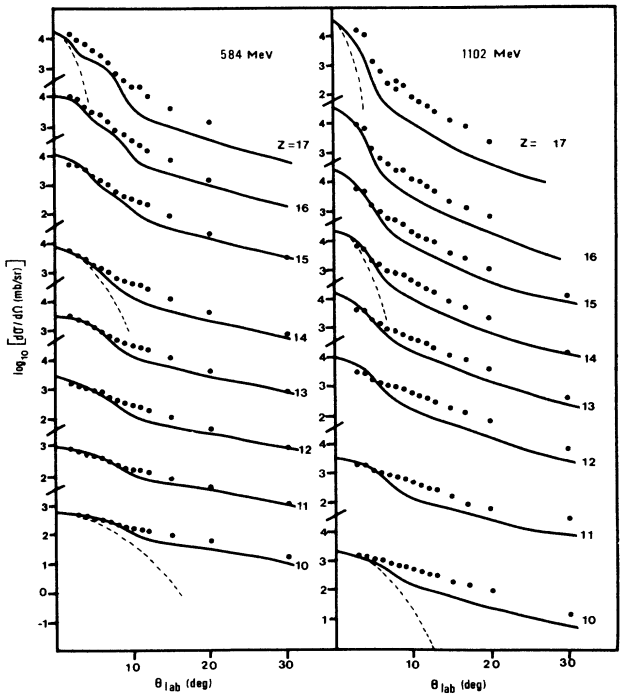

FIG. 4. (a) Angular distributions in the $^{40}Ar+^{68}Zn$ reaction at 14.6 MeV/nucleon. The solid lines are predictions as described in Sec. III B. In a few cases the distributions corresponding to recoil alone have been included for comparison (dashed lines, $\sigma_0=84$ MeV/c). (b) Same as (a), but at 27.6 MeV/nucleon (data of Refs. 1 and 18).

7° for reasons discussed in Ref. 1. However, it should not be forgotten that at 27.6 MeV/nucleon the calculation concerns only about half of the measured cross section. Thus at this energy the good agreement between the shapes of calculated and measured angular distributions may reflect a rather featureless angular distribution for the part of the cross section due to disintegration of highly excited nuclei, as is expected from kinematic considerations.

C. Energy loss

As mentioned in the Introduction, the treatment of energy spectra will be limited in this work to the calculation of the mean energy per nucleon of observed fragments as a function of laboratory angle. The kinetic energy loss is supposed, as in Ref. 8, to be due to the primary nucleon-nucleon collisions. Explicitly,

$$E_F'=E_{\rm lab}(1-1/A_p)^n , \tag{38}$$

which corresponds to a loss of the instantaneous energy per nucleon at each nucleon-nucleon collision. We may now calculate the average value of E_F'/A_F' (the primes denote primary fragments) for each primary fragment A_F' as

$$\frac{\langle E_F'\rangle}{A_F'}=\sum_n P_{A_F'}(n)(E_F'/A_F') , \tag{39}$$

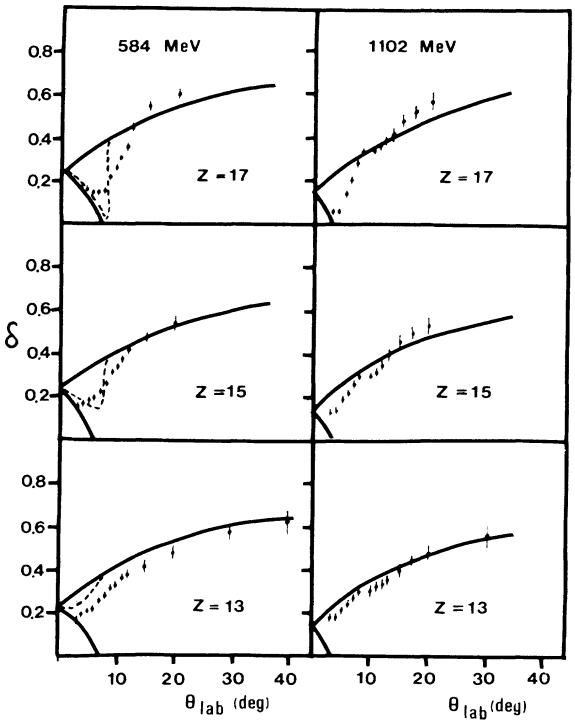

FIG. 5. Variation of the parameter δ (see text) with laboratory angle for projectile-like fragments at (a) 14.6 and (b) 27.6 MeV/nucleon. The solid curves are model predictions as described in the text. At small angles the two branches correspond to Coulomb and nuclear parts of the deflection function. At the lower energy the dashed line at small angles indicates the cross-section weighted average of δ for the two branches.

where $P_{A'_F}$ is the probability of forming a given primary fragment at a particular impact parameter (primary laboratory angle) for which there were n nucleon-nucleon collisions. We also require the probability that a given primary fragment (A'_F) leads to the final observed fragment (A_F), which enables us to calculate the average energy per nucleon as

$$\frac{\langle E_F \rangle}{A_F} = \sum_{A'_F} P_{A'_F A_F} \langle E'_F / A'_F \rangle \ . \tag{40}$$

Stated more simply, the spectrum of the energy per nucleon of the observed fragment corresponds to the contributing spectrum of primary fragments, each characterized by an average E'_F/A'_F for a given primary laboratory angle [given by Eq. (26)].

We should also comment on the energy loss due to Q-value effects. For the secondary emission this quantity is contained in Eq. (31). For the primary mass change the required correction is expected to be small if the nucleons lost from the projectile are transferred to the target (and vice versa) and larger (~ 8 MeV/nucleon) if the primary mass change is accompanied by emission of nucleons. We have, in this work, supposed the former mechanism to predominate, and have therefore included no explicit Q-value corrections.

The calculations thus based on Eqs. (38)—(40) are shown together with the data in Fig. 5, in which the mean energy loss has been characterized by the parameter

$$\delta = \left[\frac{E_p}{A_p} - \frac{\langle E_F \rangle}{A_F} \right] \Big/ (E_p/A_p) \ , \tag{41}$$

where p and F refer, as above, to the projectile and the observed fragment. It will be seen that good agreement is obtained with the data. At the lower energy the effect of the Coulomb branch of the deflection function is particularly apparent for fragments with Z close to that of the projectile. Indeed, δ initially decreases with increasing laboratory angle for $Z=17$ at $E_{\rm lab}(^{40}{\rm Ar})=584$ MeV and the effect is reproduced by the calculations. For small angles the primary energy loss is well approximated by a straight line:

$$\frac{\langle E'_F \rangle}{A'_F} = \frac{E_{\rm lab}}{A_p} \left[1 - \frac{P'_0 T}{A'_F} \right] \tag{42}$$

(this equation is exact as P_{+1} tends to zero), and provides some *a posteriori* justification for the use of Eq. (29).

IV. SUMMARY AND DISCUSSION

We have presented in this work a simple analytical model for peripheral heavy ion collisions which predicts inclusive experimental observables in a consistent manner. We have shown explicitly how to calculate mass or charge yields of projectile-like fragments and corresponding angular distributions. We also presented a limited discussion of energy loss. An application of the model to the $^{40}{\rm Ar}+^{68}{\rm Zn}$ reaction at 14.6 and 27.6 MeV/nucleon has been made. At the lower energy the model predictions agree well with the experimental measurements. At the higher energy the measured cross section for the projectile-like fragments is about twice as large as the model prediction. Despite this fact, the form of the predicted angular distributions is similar to that measured experimentally. The origin of the excess cross section has been discussed. It seems likely, in the light of the work of Barbagallo *et al.*,[19] that highly excited projectile-like fragments produced in central collisions disintegrate, producing fragments whose masses are similar to those expected from an asymmetric splitting of the primary fragment. It is not clear to what extent this second mechanism may be thought of as simply the evaporation of massive fragments as described in the work of Moretto and collaborators.[23] However, it should be remarked that at 20 MeV/nucleon coincidences between fragments with $Z>3$ have been observed in the $^{35}{\rm Cl}+{\rm Ta}$ reaction with yields estimated at a few percent of the inclusive production rates.[24] The central question is thus: Do primary projectile-like fragments with an initial temperature of 5—8 MeV evaporate light particles (in which case an ^{40}Ar nucleus would be reduced to a collection of particles with $Z<3$), or do they, on the other hand, disintegrate into two or more large fragments which, despite possible subsequent evaporation, are observed as cold products in experiments?

It is perhaps instructive to compare the present model

with those familiar at higher and lower energies. At low energies, it will be clear that the primary loss and gain probabilities P'_{-1} and P'_{+1} may be reinterpreted in terms of drift and diffusion coefficients characteristic of a diffusion process and thus may be estimated either using a macroscopic potential energy[25] or by considering the interaction of two Fermi gases.[26] There appears to be some experimental evidence that near the Coulomb barrier time dependent probabilities are required to explain the measurements.[27] On the other hand, it should not be forgotten that the absence of collective effects would probably limit the application of the present model to energies well above the Coulomb barrier. In any case it should be emphasized that the use of empirical probabilities allows us not only to include secondary emission (evaporation), but also to allow for emission of nucleons to the continuum in the primary interaction.

At high energies ($\gtrsim$ 100 MeV/nucleon) the formulation of the model leads us to expect some similarity to the abrasion-ablation approach.[28,29] In this context it should be pointed out that the presence of the inelastic probability P'_0 is, in some sense, equivalent to the final state interaction invoked by Hufner *et al.*[28] to account for discrepancies between the predictions of the abrasion-ablation model and experimental measurements. However, herein the formation of an equilibrated piece of nuclear matter (corresponding to the participant zone or fireball), is not considered. The participant zone corresponds to nucleons transferred from projectile (target) to target (projectile), to nucleons reabsorbed in their parent nuclei (or nucleon exchange) corresponding to inelastic scattering, or to nucleons emitted to the continuum. Another difference is that the dissipated energy is assumed to arise from nucleon-nucleon collisions and is not calculated as the change in surface energy due to abrasion.

Besides investigation of these topics and a more extensive treatment of energy spectra, other extensions of the model are planned. One may easily make a calculation for isotopic yields by separating the probability for nucleon loss or gain into corresponding neutron and proton probabilities. One may also calculate multiplicities and angular distributions of light emitted particles, although the calculation requires simultaneous treatment of the projectile and target masses. Finally, one can predict results of exclusive experiments (probably using a Monte Carlo representation of the model) in which light particles are observed in coincidence with the heavier projectile residues.

ACKNOWLEDGMENTS

Thanks are due the authors of Ref. 1 for making data (at 14.6 MeV/nucleon) available prior to publication and for stimulating discussions. The author would also like to acknowledge helpful comments from P. Schuck, M. Durand, and F. Rami.

[1]F. Rami, J. P. Coffin, G. Guillaume, B. Heusch, P. Wagner, A. Fahli, and P. Fintz, Nucl. Phys. **A444**, 325 (1985).
[2]Ch. Egelhaaf, G. Bohlen, H. Fuchs, A. Gamp, H. Homeyer, and H. Kluge, Phys. Rev. Lett. **46**, 813 (1981).
[3]V. Borrel, D. Guerreau, J. Galin, B. Gatty, D. Jaquet, and X. Tarrago, Z. Phys. A **314**, 191 (1983).
[4]R. Dayras, in Proceedings of the International Conference on Heavy Ion Nuclear Collisions in the Fermi Energy Domain, Caen, May 1986.
[5]G. K. Gelbke, D.K. Scott, M. Bini, D. L. Hendrie, J. L. Laville, J. Mahoney, M. C. Mermaz, and C. Olmer, Phys. Lett. **70B**, 415 (1977).
[6]K. Van Bibber, D. L. Hendrie, D. K. Scott, H. H. Weiman, L. S. Schroeder, J. V. Geaga, S. A. Cessin, R. Treuhaft, Y. J. Grossiord, J. O. Rasmussen, and C. Y. Wong, Phys. Rev. Lett. **43**, 840 (1979).
[7]A. S. Goldhaber, Phys. Lett. **53B**, 306 (1984).
[8]A. J. Cole, Z. Phys. A **322**, 315 (1985).
[9]X. Campi, J. Debois, and E. Lipparini, Phys. Lett. **142B**, 8 (1984).
[10]W. Czyz and L. C. Maximon, Ann. Phys. (N.Y.) **52**, 59 (1969).
[11]B. G. Harvey, Nucl. Phys. **A444**, 498 (1985).
[12]P. J. Karol, Phys. Rev. C **11**, 1203 (1975).
[13]G. W. Greenless, G. J. Pyle, and Y. C. Tang, Phys. Rev. **171**, 1115 (1968).
[14]R. W. Hasse and P. Schuck, Nucl. Phys. **A438**, 157 (1985).
[15]A. J. Cole, N. Longequeue, J. Menet, J. J. Lucas, R. Ost, and J. B. Viano, Nucl. Phys. **A341**, 284 (1980).
[16]F. Puhlhofer, Nucl. Phys. **A280**, 267 (1977).
[17]B. Fernandez, C. Gaarde, J. S. Larsen, S. Pontopiddan, and F. Vidbaek, Nucl. Phys. **A306**, 259 (1978).
[18]F. Rami, 3ieme cycle thesis, Centre Recherches Nucleaires—Strasbourg, 1985 (unpublished) and private communication.
[19]C. Barbagallo, J. Richert, and P. Wagner, Z. Phys. A **324**, 97 (1986).
[20]A. J. Cole, contribution to Workshop on Hot Nuclei and Nuclear Disassembly, Grenoble, 1986 (unpublished).
[21]J. Bondorf, R. Donangelo, I. N. Mishutin, and H. Schulz, Nucl. Phys. **A444**, 460 (1985).
[22]R. W. Hasse and P. Schuck, Nucl. Phys. **A445**, 205 (1985); P. Schuck, private communication.
[23]L. G. Moretto, Phys. Lett. **40B**, 185 (1972); L. G. Sobotka, M. L. Padgett, G. J. Wozniak, G. Guarino, A. J. Pacheco, L. G. Moretto, Y. Chan, R. G. Stokstad, T. Tseruya, and S. Wald, Phys. Rev. Lett. **51**, 2187 (1983).
[24]M. J. Murphy, D. Leach, A. Ray, A. Seamster, and R. Vandenbosch, Phys. Rev. C **33**, 165 (1986).
[25]L. G. Moretto and J. S. Sventek, Phys. Lett. **58B**, 26 (1975); L. G. Moretto, R. P. Babinet, J. Galin, and S. G. Thompson, *ibid.* **58B**, 31 (1975).
[26]J. Randrup, Nucl. Phys. **A327**, 490 (1979).
[27]K. E. Rehm, H. Essel, K. Hortel, P. Kienle, H. J. Korner, P. Sperr, and W. Wagner, Phys. Lett. **86B**, 256 (1977); K. E. Rehm, *ibid.* **86B**, 260 (1977).
[28]J. Hüfner, K. Schafer, and B. Shurman, Phys. Rev. C **12**, 1888 (1975).
[29]J. D. Bowman, W. J. Swiatecki, and C. F. Tsang, Lawrence Berkeley Laboratory Internal Report No. LBL-2908, 1973 (unpublished).